Supporting Information:

Nanoparticle ligand density measurement and analysis: Nanoparticle suspensions were centrifuged (14.5 kxg, minimum 60 min) to pellet particles, and the supernatant was removed and the particles were re-suspended and sonicated in a small amount of 18 $M\Omega$ cm deionized water (Barnsted Nanopure). Particles were dripped onto pre-cleaned highly conductive (<1 milliohm-cm) silicon wafers and dried in at least two iterations. The nanoparticle layers were sufficiently thick that the underlying Si wafer was not detectable in subsequent XPS measurements. In order to validate the procedures used to correct the data for electron scattering, we also prepared "ligand-free" samples by gently removing the ligands by photo-oxidation. XPS measurements were performed using a custom-built, ultra-high vacuum Physical Electronics XPS system equipped with an aluminum Kα source (~ 1487 eV x-ray energy), a quartz-crystal X-ray monochromator, a hemispherical electron energy analyzer, and a 16-channel array detector. This system is ion-pumped with a base pressure of $<2x10^{-10}$ torr. For each ligand, XPS spectra were obtained, and initial experiments were used to determine which specific peaks provided the best quantitative data free of extraneous contamination. Subsequent experiments involved measuring and quantitatively analyzing these peaks. For CTAB and PAH-modified nanoparticles, the C(1s) /Au peak area ratio was used for quantitative primary analysis. For MPA, the S(2p) peak was used because the C(1s) signal from this small molecule is otherwise difficult to separate unambiguously from potential background contamination. For citrate, we used

the high binding-energy carbon peak near 290 eV that is characteristic of carboxylic acid groups; typical contamination shows little or no signal in this region.

Nanoparticle shape and inelastic scattering within the Au and within the inorganic layer accounted for using direct finite-element analysis to model the creation and scattering of electrons within ligand-coated spherical nanoparticles [1]To account for the electron scattering within the organic layers, values for the inelastic mean free paths (IMFP) measured by Laibinis, et al[2] for Au photoelectrons propagating through self-assembled alkyl monolayers of different thicknesses, yielding values for the IMFP of ~ 1400 eV for Au photoelectrons propagating through the organic monolayers $\lambda_{Au,C}$. The IMFP of the ~ 1200 eV C(1s) electrons scattering within the organic film were then obtained using the well-known energy scaling laws, [3] and these values were used as inputs into the finite-element analysis program to model the experimentally observed XPS peak ratios as a function of ligand coverage. As a check, we also compared the absolute intensity of the Au XPS peaks from ligand-covered and the "ligand-free" samples prepared by ozone oxidation of the ligand-covered samples, as described above. Measuring the absolute Au peak areas from the ligand-free sample ($A_{ligand\text{-}free}$) and ligand-bearing samples ($A_{ligand\text{-}bearing}$) with identical sample geometry and alignment yields a direct measure of the $t/\lambda_{Au,C}$ via

$$\frac{A_{ligand-bearing}}{A_{ligand-free}} = \exp^{-t/\lambda_{Au,C}}$$

where t is the thickness of the film and the $\lambda_{Au,C}$ is the inelastic mean free path of Au electrons in the organic layer. In all cases where a direct comparison could be made, we found that the finite-element modeling yielded results consistent with the experimental data.

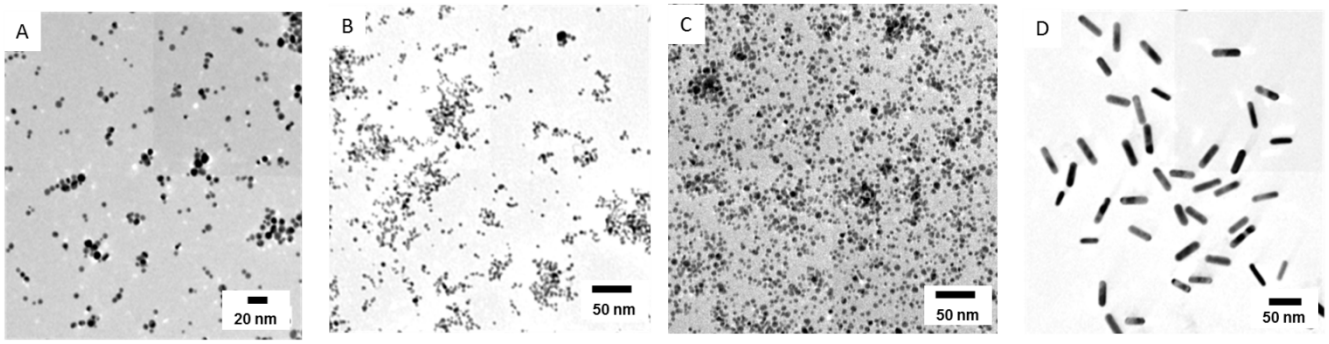

Figure S1. Representative TEM images of functionalized AuNPs used in this study. **(A)** 4.7 nm PAH-AuNPs, scale bar 20 nm. **(B)** 4.9 nm Cit-AuNPs, scale bar 50 nm. **(C)** 3.8 nm MPA-AuNPs, scale bar 50 nm. **(D)** 50x12 nm CTAB-AuNRs, scale bar 50 nm.

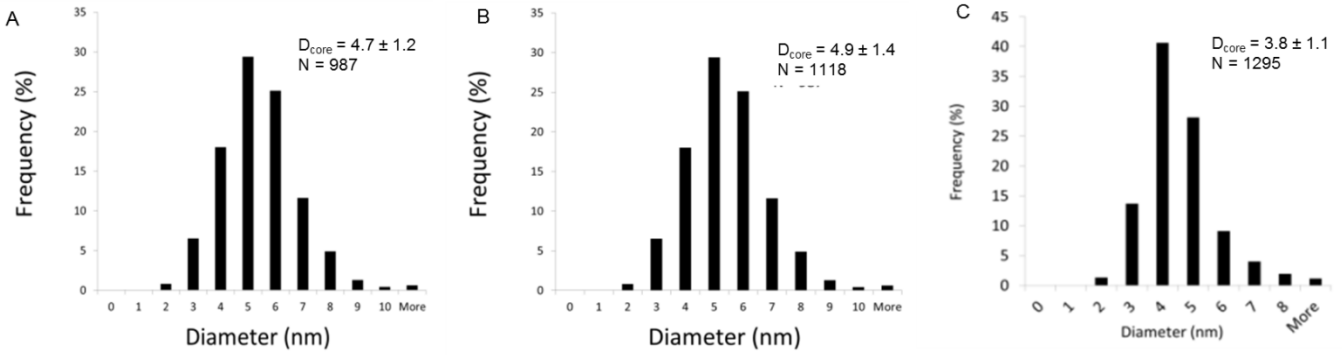

Figure S2. Size distribution data for the spherical AuNPs used in the study. **(A)** 4.7 nm PAH-AuNPs. **(B)** 4.9 nm Cit-AuNPs. **(C)** 3.8 nm MPA-AuNPs.

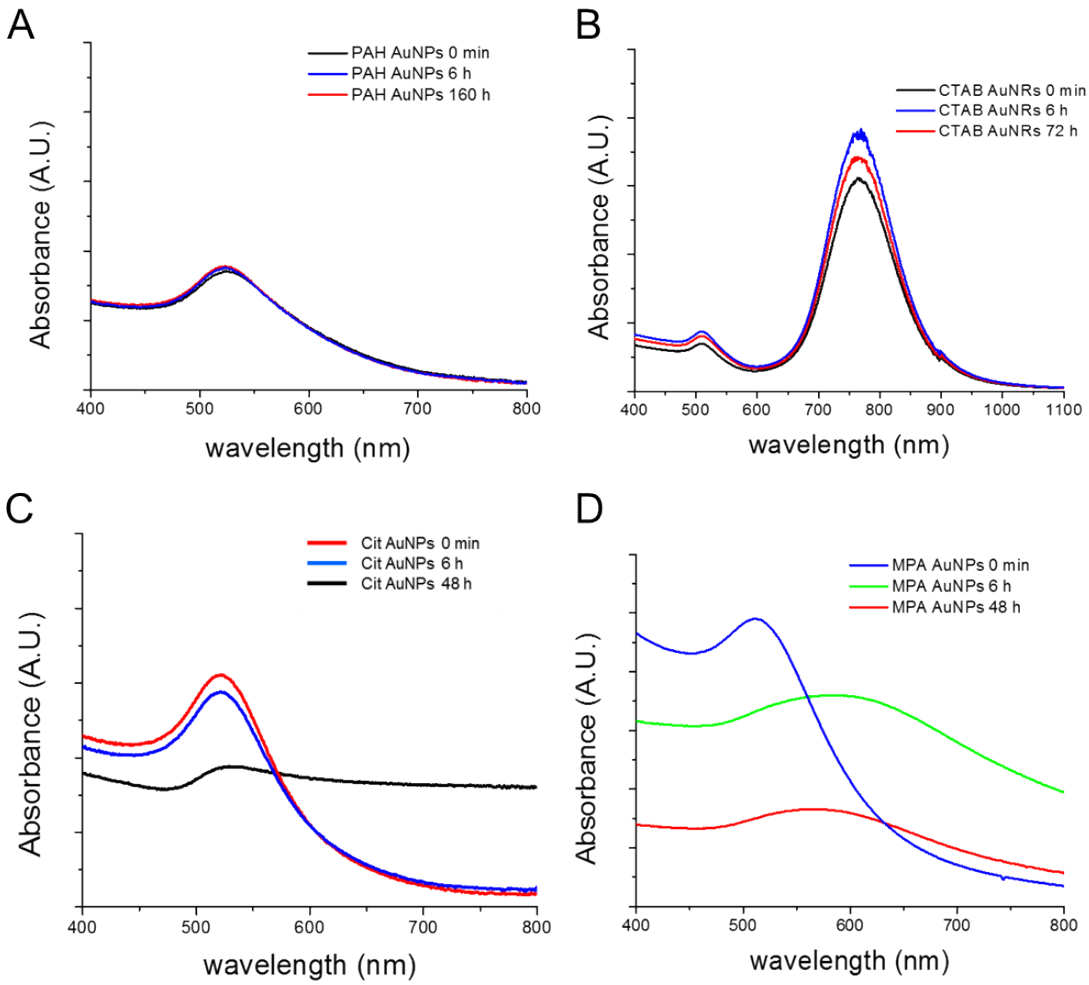

Figure S3. UV-vis spectroscopy analysis of AuNP stability in *Daphnia* media over an extended period of time. Exposure conditions mirror the acute toxicity exposures. **(A)** PAH-AuNPs, **(B)** CTAB-AuNRs, **(C)** Cit-AuNPs, and **(D)** MPA-AuNPs. [AuNP] = 10.0 nM, [CTAB-AuNR] = 2.0 nM.

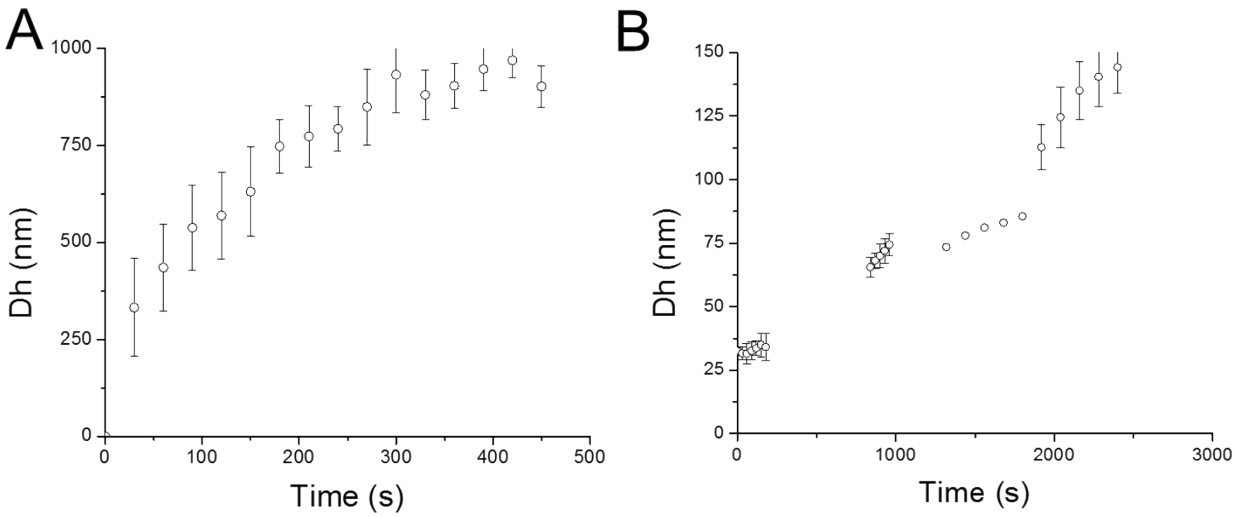

Figure S4. DLS analysis of **(A)** MPA-AuNP aggregation and **(B)** Cit-AuNP aggregation in *Daphnia* media over various incubation times. Incubation conditions mirrored the acute toxicity exposures. [AuNP] = 10.0 nM.

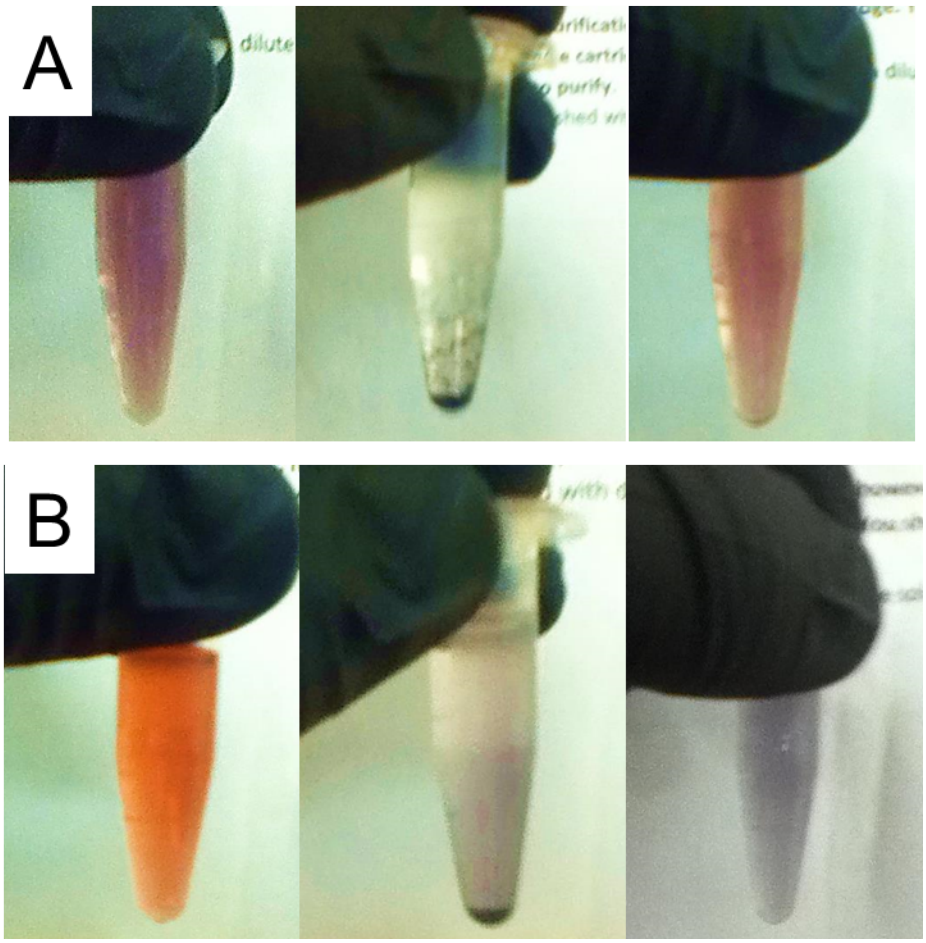

Figure S5. Negatively-charged AuNPs (Cit, MPA-AuNPs) aggregate over 48 h in Daphnia media, however the MPA-AuNPs and the Cit-AuNPs show different aggregation behaviors. (A) MPA-AuNPs aggregate reversibly. After 48 hours, the initial red-brown solution (left) gives way to black clumps of aggregated AuNPs (middle), but after gentle agitation, the red-brown solution color is restored (right). (B) In contrast, Cit-AuNPs aggregate irreversibly. The red-orange solution (left) gives way to a black-blue aggregate (middle). Even after vortex mixing and sonication, the solution remains blue-black; the AuNPs have not re-suspended.

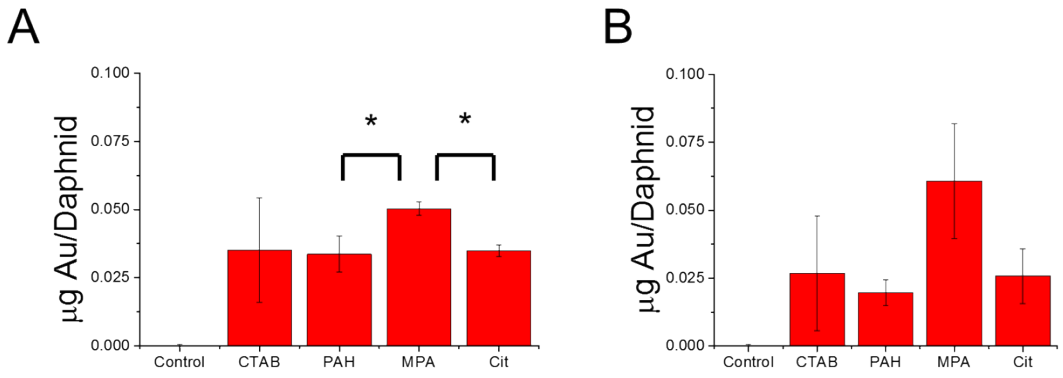

Figure S6. *Daphnia* ICP-MS uptake data for AuNPs used in the study. Difference between the AuNP uptake in *Daphnia* (A) vs the uptake after iodide etching with a 100mM iodide solution (B). Asterix indicate significant difference ($p < 0.05$) between treatments marked by bracket.

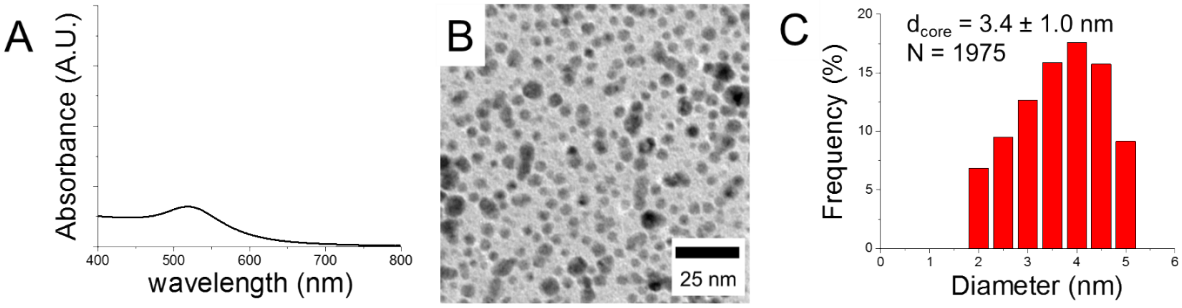

Figure S7. UV-vis absorption spectrum **(A)** of the PAH-AuNP supernatant. Representative TEM image **(B)** of the concentrated PAH-AuNP supernatant, and the corresponding size distribution analysis **(C)**.

1. Y. Tan, S. Jin and R. J. Hamers, *Journal of Physical Chemistry C*, 2013, **117**, 313-320.
2. P. E. Laibinis, C. D. Bain and G. M. Whitesides, *Journal of Physical Chemistry*, 1991, **95**, 7017-7021.
3. S. Tanuma, C. J. Powell and D. R. Penn, *Surface and Interface Analysis*, 1993, **20**, 77-89.